



XXVIIth International Conference on Ultrarelativistic Nucleus-Nucleus Collisions
(Quark Matter 2018)

Measurements of the chiral magnetic effect with background isolation in 200 GeV Au+Au collisions at STAR

Jie Zhao (for the STAR collaboration)

Department of Physics and Astronomy, Purdue University, West Lafayette, IN, 47906, USA

Abstract

Using two novel methods, pair invariant mass (m_{inv}) and comparative measurements with respect to reaction plane (Ψ_{RP}) and participant plane (Ψ_{PP}), we isolate the possible chiral magnetic effect (CME) from backgrounds in 200 GeV Au+Au collisions at STAR. The invariant mass method identifies the resonance background contributions, coupled with the elliptic flow (v_2), to the charge correlator CME observable ($\Delta\gamma$). At high mass ($m_{inv} > 1.5 \text{ GeV}/c^2$) where resonance contribution is small, we obtain the average $\Delta\gamma$ magnitude. In the low mass region ($m_{inv} < 1.5 \text{ GeV}/c^2$), resonance peaks are observed in $\Delta\gamma(m_{inv})$. An event shape engineering (ESE) method is used to model the background shape in m_{inv} to extract the potential CME signal at low m_{inv} . In the comparative method, the Ψ_{RP} is assessed by spectator neutrons measured by ZDC, and the Ψ_{PP} by the 2nd-harmonic event plane measured by the TPC. The v_2 is stronger along Ψ_{PP} and weaker along Ψ_{RP} ; in contrast, the magnetic field, mainly from spectator protons, is weaker along Ψ_{PP} and stronger along Ψ_{RP} . As a result, the $\Delta\gamma$ measured with respect to Ψ_{RP} and Ψ_{PP} contain different amounts of CME and background, and can thus determine these two contributions. It is found that the possible CME signals with background isolation by these two novel methods are small, on the order of a few percent of the inclusive $\Delta\gamma$ measurements.

Keywords: QCD, heavy-ion collisions, chiral magnetic effect, invariant mass, reaction plane, participant plane

1. Introduction

Quark interactions with topological gluon fields can induce chirality imbalance and local parity violation in quantum chromodynamics (QCD) [1]. In relativistic heavy-ion collisions, this can lead to observable electric charge separation along the strong magnetic field, \vec{B} , produced by spectator protons [2]. This is called the chiral magnetic effect (CME). The commonly used observable to search for the CME-induced charge separation is the three-point azimuthal correlator difference [3], $\Delta\gamma \equiv \gamma_{OS} - \gamma_{SS}$; $\gamma = \langle \cos(\phi_\alpha + \phi_\beta - 2\Psi_{RP}) \rangle \approx \langle \cos(\phi_\alpha + \phi_\beta - 2\phi_c) \rangle / v_2$, where ϕ_α and ϕ_β are the azimuthal angles of two charged particles, of opposite electric charge sign (OS) or same sign (SS), and Ψ_{RP} is that of the reaction plane (span by the impact parameter direction and the beam) to which \vec{B} is perpendicular on average. The latter is often surrogated by the azimuthal angle of a third particle, ϕ_c , with a resolution correction factor given by the particle's elliptic anisotropy (v_2). Significant $\Delta\gamma$ has indeed been observed in heavy-ion collisions [4]. One

of the difficulties in its CME interpretation is a major background contribution arising from the coupling of resonance decay correlations and the v_2 stemming from the participant geometry [5–9].

2. Invariant mass dependence of the $\Delta\gamma$ correlator

The main backgrounds for the $\Delta\gamma$ are from the resonance decays coupled with v_2 . A new analysis approach exploiting the particle pair invariant mass, m_{inv} , to identify the backgrounds and, hence, to extract the possible CME signal is proposed [10]. Figure 1 (left panel) shows the m_{inv} dependence of the relative excess of OS over SS charged π pairs, $r = (N_{OS} - N_{SS})/N_{OS}$, and (middle panel) shows the m_{inv} dependence of the three-point correlator difference, $\Delta\gamma = \gamma_{OS} - \gamma_{SS}$. A lower cut on m_{inv} was used to suppress the resonance contributions. Figure 1 (right panel) shows the inclusive $\Delta\gamma$ over all mass (black) and at $m_{inv} > 1.5 \text{ GeV}/c^2$ (red) as a function of centrality in Au+Au collisions at 200 GeV. In 20-50% collisions centrality, combining results from Run-11 (~0.5 billion minimum-bias events, year 2011), Run-14 (~0.8 billion, year 2014) and Run-16 (~1.2 billion, year 2016), the $\Delta\gamma$ at $m_{inv} > 1.5 \text{ GeV}/c^2$ is $(5 \pm 2 \pm 4)\%$ of the inclusive $\Delta\gamma$.

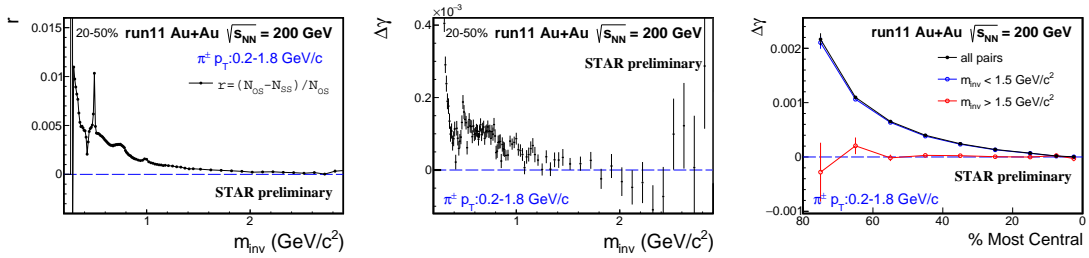


Fig. 1. Pair invariant mass, m_{inv} , dependence of the relative excess of OS over SS pairs, $r = (N_{OS} - N_{SS})/N_{OS}$ (left panel), three-point correlator difference, $\Delta\gamma = \gamma_{OS} - \gamma_{SS}$ (middle panel). (Right panel) The inclusive $\Delta\gamma$ over all mass (black) and at $m_{inv} > 1.5 \text{ GeV}/c^2$ (red) as a function of centrality. The π are identified by STAR TPC and TOF with p_T from 0.2 to 1.8 GeV/c .

The CME is expected to be a low p_T phenomenon [11]; its contribution to high mass may be small. To extract CME at low mass, resonance contributions need to be subtracted. The inclusive $\Delta\gamma$ can be expressed as $\Delta\gamma(m_{inv}) = r(m_{inv}) \times \cos(\phi_\alpha + \phi_\beta - 2\phi_{reso.}) \times v_{2,reso.} + \Delta\gamma_{CME}$ [10]. The event shape engineering (ESE) [12] method provides a tool to select events with different v_2 values by cutting on the q_2 ($\bar{q}_2 = 1/N \times \sum(\cos(2\phi), \sin(2\phi))$). The difference of the $\Delta\gamma(m_{inv})$ from different q_2 classes can be regarded as the background $\Delta\gamma(m_{inv})$ shape [13], assuming the CME are the same for events from different q_2 classes.

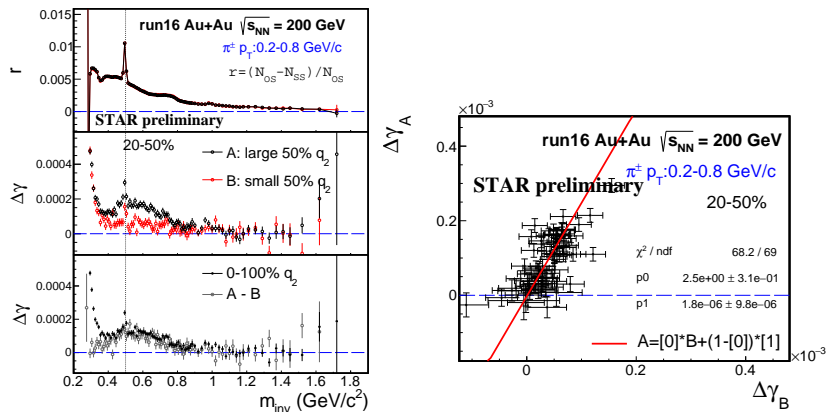


Fig. 2. Pair invariant mass, m_{inv} , dependence of the $r = (N_{OS} - N_{SS})/N_{OS}$ (left top). The $\Delta\gamma(m_{inv})$ from ESE selected event sample A (large 50% q_2) and B (small 50% q_2) (left middle). The inclusive (0-100% q_2) $\Delta\gamma$ compared with the difference between $\Delta\gamma$ from event sample A and B ($\Delta\gamma_A - \Delta\gamma_B$) (left bottom). (Right panel) $\Delta\gamma_A$ vs. $\Delta\gamma_B$ fitted by a linear function. The π are identified by STAR TPC with p_T from 0.2 to 0.8 GeV/c .

Figure 2 (left top) shows the m_{inv} dependence of the $r = (N_{OS} - N_{SS})/N_{OS}$, (left middle) shows the $\Delta\gamma(m_{inv})$ from ESE selected event sample A (large 50% q_2) and B (small 50% q_2). The correlators are calculated by $\gamma = \cos(\phi_\alpha + \phi_\beta - 2\phi_c)/v_{2,c}$. The TPC full-event is divided into east and west sub-event, with α, β and q_2 from one sub-event and c from other sub-event. Figure 2 (left bottom) shows the inclusive (0-100% q_2) $\Delta\gamma$ compared with the $\Delta\gamma$ difference between event samples A and B. A linear function, $\Delta\gamma_A = b \times \Delta\gamma_B + (1 - b) \times \Delta\gamma_{CME}$, is used to extract the CME. Figure 2 (right) shows the fit result. Combining Runs 11, 14 and 16, the fit parameter $\Delta\gamma_{CME}$ is $(2 \pm 4 \pm 6)\%$ of inclusive $\Delta\gamma$ in 20-50% centrality Au+Au collisions.

3. $\Delta\gamma$ with respect to Ψ_{RP} (ZDC) and Ψ_{PP} (TPC)

The CME-driven charge separation is along the magnetic field direction (Ψ_B). The major background to the CME is related to the elliptic flow anisotropy (v_2), determined by the participant geometry. A novel idea of differential measurements with respect to the reaction plane (Ψ_{RP}) and participant plane (Ψ_{PP}) is proposed [14, 15], where the Ψ_{RP} could be assessed by spectator neutrons measured by the zero-degree calorimeters (ZDC) [16]. The v_2 is stronger along Ψ_{PP} and weaker along Ψ_{RP} ; in contrast, the magnetic field, being from spectator protons, is weaker along Ψ_{PP} and stronger along Ψ_{RP} . The $\Delta\gamma$ measured with respect to Ψ_{RP} and Ψ_{PP} contain different amounts of CME and background, and can thus determine these two contributions assuming the CME is proportional to the magnetic field squared and background is proportional to v_2 [14]:

$$\begin{aligned} \Delta\gamma\{\Psi_{TPC}\} &= \Delta\gamma_{CME}\{\Psi_{TPC}\} + \Delta\gamma_{Bkg}\{\Psi_{TPC}\}, \Delta\gamma\{\Psi_{ZDC}\} = \Delta\gamma_{CME}\{\Psi_{ZDC}\} + \Delta\gamma_{Bkg}\{\Psi_{ZDC}\}, \\ \Delta\gamma_{CME}\{\Psi_{TPC}\} &= a * \Delta\gamma_{CME}\{\Psi_{ZDC}\}, \Delta\gamma_{Bkg}\{\Psi_{ZDC}\} = a * \Delta\gamma_{Bkg}\{\Psi_{TPC}\}, \\ a &= v_2\{\Psi_{ZDC}\}/v_2\{\Psi_{TPC}\}, A = \Delta\gamma\{\Psi_{ZDC}\}/\Delta\gamma\{\Psi_{TPC}\}, \\ f_{CME}^{EP} &= \Delta\gamma_{CME}\{\Psi_{TPC}\}/\Delta\gamma\{\Psi_{TPC}\} = (A/a - 1)/(1/a^2 - 1). \end{aligned} \quad (1)$$

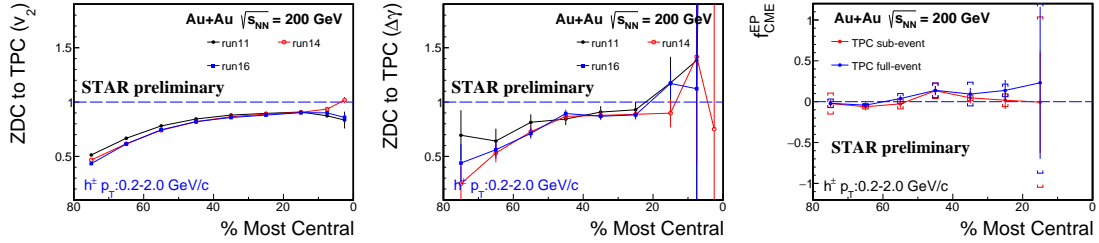


Fig. 3. The centrality dependences of the ratios of the v_2 (left panel) and $\Delta\gamma$ (middle panel) measured with respect to the ZDC event plane to those with respect to the TPC event plane. (Right panel) The extracted f_{CME}^{EP} as a function of collision centrality.

Figure 3 shows the ratio of v_2 (left) measured with respect to the ZDC event plane and the v_2 with respect to the TPC event plane, $a = v_2\{\Psi_{ZDC}\}/v_2\{\Psi_{TPC}\}$ in Eq. 1, and that of $\Delta\gamma$ (middle panel), $A = \Delta\gamma\{\Psi_{ZDC}\}/\Delta\gamma\{\Psi_{TPC}\}$ in Eq. 1, as functions of collisions centrality. To suppress the non-flow contributions in v_2 and $\Delta\gamma$ measurements, the TPC sub-event method is used, where each TPC event is divided into east and west sub-event, with event-plane from one sub-event and particles of interest from the other sub-event. Figure 3 (right) show the extracted possible CME fraction (f_{CME}^{EP}) [14] as function of centrality. For comparison the results from TPC full-event method are also plotted. The extracted f_{CME}^{EP} (combined from Runs 11, 14 and 16) are $(9 \pm 4 \pm 7)\%$ and $(12 \pm 4 \pm 11)\%$ from the TPC sub-event and full-event methods in 20-50% centrality Au+Au collisions, respectively.

4. Summary

Charge separation measurements by the three-point azimuthal correlator ($\Delta\gamma$) are contaminated by major backgrounds arising from resonance decay correlations coupled with the elliptical anisotropy (v_2). To

reduce/eliminate background contaminations, two novel methods are employed: the $\Delta\gamma$ correlator as a function of the particle pair invariant mass (m_{inv}) and the comparative $\Delta\gamma$ measurements with respect to Ψ_{RP} (estimated by ZDC) and Ψ_{PP} (estimated by TPC).

Resonance structures are observed in $\Delta\gamma$ as function of π - π m_{inv} . A lower m_{inv} cut ($m_{inv} > 1.5$ GeV/ c^2) yields a $\Delta\gamma$ fraction of $(5 \pm 2 \pm 4)\%$ of the inclusive $\Delta\gamma$ measurement. In the low mass region, event shape engineering is used to determine the background shape in m_{inv} , and a linear fit to $\Delta\gamma(m_{inv})$ yields a possible CME signal of $(2 \pm 4 \pm 6)\%$ of the inclusive $\Delta\gamma$ measurement in 20-50% centrality Au+Au collisions.

The $\Delta\gamma$ measurements with respect to Ψ_{RP} and Ψ_{PP} contain different amounts of CME and background. The v_2 is stronger along Ψ_{PP} and weaker along Ψ_{RP} ; and the magnetic field is weaker along Ψ_{PP} and stronger along Ψ_{RP} . By comparing the v_2 and $\Delta\gamma$ with respect to Ψ_{RP} and Ψ_{PP} , the extracted possible CME fractions are $(9 \pm 4 \pm 7)\%$ and $(12 \pm 4 \pm 11)\%$ from the TPC sub-event and full-event methods in 20-50% centrality Au+Au collisions, respectively.

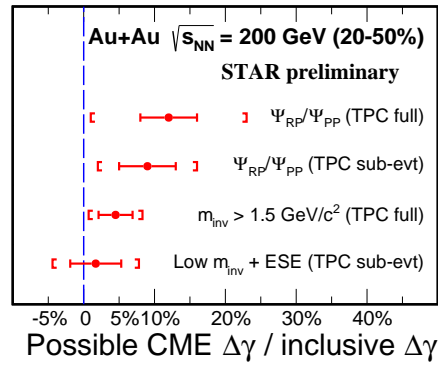


Fig. 4. The possible CME $\Delta\gamma$ over the inclusive $\Delta\gamma$ fraction from different analysis methods in middle central (20-50%) Au+Au collisions at $\sqrt{s_{NN}} = 200$ GeV.

The extracted potential CME signal fraction (CME $\Delta\gamma$ over the inclusive $\Delta\gamma$) in middle central (20-50%) Au+Au collisions at $\sqrt{s_{NN}} = 200$ GeV are summarized in Fig. 4. These data-driven estimates indicate that the possible CME signal is small, within 1-2 σ from zero. Precision can be improved in the future with more Au+Au data and the new isobar data. Possible ZDC upgrades to achieve better RP determination are being investigated.

Acknowledgments This work was partly supported by the U.S. Department of Energy (Grant No. de-sc0012910), and the NSFC of China under Grant No. 11505073.

References

- [1] D. Kharzeev, R. D. Pisarski, M. H. G. Tytgat, Phys. Rev. Lett. 81 (1998) 512–515.
- [2] K. Fukushima, D. E. Kharzeev, H. J. Warringa, Phys. Rev. D78 (2008) 074033.
- [3] S. A. Voloshin, Phys. Rev. C70 (2004) 057901.
- [4] D. E. Kharzeev, J. Liao, S. A. Voloshin, G. Wang, Prog. Part. Nucl. Phys. 88 (2016) 1–28.
- [5] F. Wang, Phys.Rev. C81 (2010) 064902.
- [6] A. Bzdak, V. Koch, J. Liao, Phys.Rev. C81 (2010) 031901.
- [7] S. Schlichting, S. Pratt, Phys.Rev. C83 (2011) 014913.
- [8] L. Adamczyk, et al., Phys. Rev. C89 (4) (2014) 044908.
- [9] F. Wang, J. Zhao, Phys. Rev. C95 (5) (2017) 051901 (R).
- [10] J. Zhao, H. Li, F. Wang, arXiv: 1705. 05410.
- [11] D. E. Kharzeev, L. D. McLerran, H. J. Warringa, Nucl. Phys. A803 (2008) 227–253.
- [12] J. Schukraft, A. Timmins, S. A. Voloshin, Phys. Lett. B719 (2013) 394–398.
- [13] J. Zhao, Int. J. Mod. Phys. A33 (13) (2018) 1830010.
- [14] H. Xu, J. Zhao, X. Wang, H. Li, Z. Lin, C. Shen, F. Wang, Chin. Phys. C 42 (2018) 084103.
- [15] H. Xu, X. Wang, H. Li, J. Zhao, Z. Lin, C. Shen, F. Wang, Phys. Rev. Lett. 121 (2018) 022301.
- [16] C. Adler, H. Strobele, A. Denisov, E. Garcia, M. Murray, S. White, Nucl. Instrum. Meth. A461 (2001) 337–340.